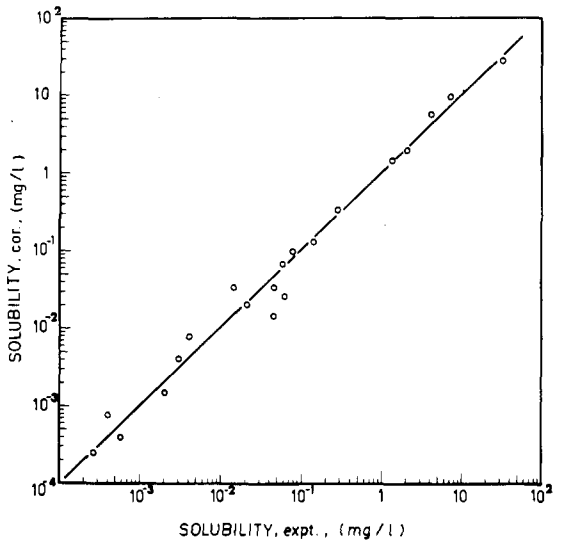

Figure 3. Comparison of correlated and experimental solubilities.

such compounds one procedure is to calculate γ for the PNA of equal carbon number, then multiply this value by about 2.0, effectively halving the solubility. An alternative procedure is to follow the approach of Pierotti et al. (*5*) and calculate the activity coefficient of the parent (unsubstituted) hydrocarbon for alkylbenzenes, then increase log γ by 0.622, i.e., a factor of 4.2 on γ, for each alkyl carbon present. The correlation obtained is shown in Figure 2 and has the form

$$\log \gamma_w^\infty = 3.5055 + 0.3417(N - 6) - 0.002640(N - 6)^2 \quad (4)$$

where N is carbon number. Correlated and experimental values of solubility excluding the alkyl subsituted naphthalenes and anthracenes are compared in Figure 3. The average deviation in log solubility is about 0.26 which corresponds to a factor of 1.8 but in some cases the deviation may be as high as a factor of 3. Although these deviations are large, the calculated solubilities are sufficiently accurate for many environmental calculation purposes. Since the correlation extends over 5 orders of magnitude and uses only carbon number and melting point, the accuracy is regarded as satisfactory. More accurate correlations will probably be developed when more thermal, solubility, and volumetric data are available for these compounds.

In conclusion, aqueous solubility data have been obtained for 32 PNA and indan. For approximate solubility estimation, the best procedure presently available for liquid hydrocarbons is to calculate γ_w^∞ from eq 4. The mole fraction solubility is then the reciprocal of γ_w^∞. For solid hydrocarbons (i.e., melting point above 25 °C) γ^∞ can be calculated from eq 4, (f_s/f_r) from eq 3, and the solubility then calculated from eq 2. For alkyl-substituted naphthalenes or anthracenes the correlated solubilities are about double the experimental values and a correction of this magnitude is needed for such compounds.

Literature Cited

(1) Bohon, R. L., Claussen, W. F. *J. Am. Chem. Soc.*, **73,** 1571 (1951).
(2) Davis, W. W., Krahl, M. E., Clowes, G. H. A. *J. Am. Chem. Soc.*, **64,** 108 (1942).
(3) Klevens, H. B. *J. Phys. Colloid. Chem.*, **54,** 283 (1950).
(4) Leinonen, P. J., Mackay, D., Phillips, C. R., *Can. J. Chem. Eng.*, **49,** 288 (1971).
(5) Pierotti, G. J., Deal, C. H., Derr, E. L. *Ind. Eng. Chem.*, **51,** 95 (1959).
(6) Schwarz, F. P., Wasik, S. P. National Bureau of Standards, Washington, D.C., personal communication.
(7) Tsonopoulos, C., Prausnitz, J. M. *Ind. Eng. Chem. Fundam.*, **10,** 593 (1971).
(8) Wauchope, R. D., Getzen, F. W. *J. Chem. Eng. Data*, **17,** 38 (1972).
(9) Weimer, R. F., Prausnitz, J. M. *J. Chem. Phys.*, **42,** 3643 (1965).

Received for review November 29, 1976. Accepted June 27, 1977. The financial support of the Inland Waters Directorate of Environment Canada and the National Research Council of Canada is gratefully acknowledged.

Vapor–Liquid Equilibrium of the Methane–*n*-Hexane System at Low Temperature

Yueh-Neu Lin, Roger J. J. Chen, Patsy S. Chappelear, and Riki Kobayashi*
Department of Chemical Engineering, William Marsh Rice University, Houston, Texas 77001

Measurements of the bubble-point compositions are reported and combined with earlier dew-point data from this laboratory to give *K* values for the methane–*n*-hexane system at seven temperatures, 0, −25, −50, −63, −75, −80, and −82.65 °C, from 20 up to 2675 psia. The data may also be evaluated isobarically without interpolation. Two liquid phases were observed in the temperature region between −77.24 (UCST) and −90.69 °C (LCST); detailed *composition measurements were made over this entire* three-phase region and associated two-phase regions at a total of five temperatures. Equilibrium constants are reported for all three binaries encountered: G–L_1, G–L_2, and L_1–L_2.

A number of studies of the vapor–liquid equilibrium of the methane–*n*-hexane binary system have been reported in the literature. Both liquid and gas phases were studied by Boomer and Johnson (*1*) at 25, 55, and 85 °C and by Poston and McKetta (*9*) over the range 100–340 °F. The lowest temperatures were studied by Shim and Kohn (*11*) in the range −110 to 150 °C, but they did not measure dew points below 0 °C or any bubble points near the critical pressure. Shim and Kohn did not report the two liquid phases existing at temperatures between −77.24 and −90.69 °C. Davenport and Rowlinson (*7*) reported, in a study of hydrocarbon solubilities in methane, that the methane–*n*-hexane system exhibited limited immiscibility, with an LCST of −90.6 °C. Earlier dew point studies in this laboratory (*5*) defined the three-phase region.

Experimental K values, obtained by combining the vapor-phase measurements of the elution method (*5*) with those obtained for the liquid phases by use of gas chromatography measurements, are presented here for the CH_4–*n*-C_6H_{14} binary system. Equilibrium constants κ between the liquids for each component in this system are also evaluated.

Experimental Method and Procedure

The recycle equilibrium apparatus is the same as used by Elliot et al. (*8*) in the methane–*n*-butane investigation with some modifications. The boiling point of *n*-hexane is 68.95 °C.

Table I. Comparison of Dew Points Measured by the Elution and Chromatographic Methods

Temp, °C (°F)	Pressure, psia	Pressure, kPa[b]	Methane mole fraction	
			y	y^a
0.01				
(32.02)	20.1	138.58	0.9550	0.9558
	25.1	173.06	0.9623	0.9643
	50.1	345.43	0.9804	0.9815
	100.1	690.16	0.9872	0.9898
	150.1	1034.90	0.9916	0.9927
−50.00	1600	11032	0.9890	0.9841
(−58.00)				

[a] Experimental "elution" dew-point data from Chen et al. (*5*). [b] Pa: Pascal = kg/m s^2 = N/m^2; 1 psia = 6.8947 kPa.

Therefore the problem of nonhomogeneous evaporation of the liquid phase in the sample line was more pronounced in this work than those encountered in the methane–*n*-butane (*8*) and methane–*n*-pentane systems (*6*). The temperature of the sampling lines was kept at more than 100 °C to transform and keep the sample in the vapor phase at essentially atmospheric conditions. A stirred pot with a volume of approximately 150 mL was used to homogenize the sample of the liquid phase (as a vapor) by mixing.

The experimental equipment and technique for the dew-point concentration data have been reported in detail in earlier publications (*3–5*) which should be consulted for itemized information.

In this bubble-point concentration investigation, a Barber-Coleman Gas Chromatograph Series 5000 Selecta System with flame ionization detection was used for analysis. The chromatographic column was a 4-ft length of $\frac{1}{8}$ in. o.d. stainless steel tubing packed with 80–100 mesh Duropak (OPN/PORASIL C). Helium was used as a carrier gas. The flow rates of air and hydrogen were determined to give maximum response. Sample was introduced into the sample loop and then bubbled through a water column to indicate the flow rate of the sample. The signal from the detector was integrated by an Autolab Model 6300 digital integrator and recorded on a Leeds and Northrup strip chart recorder. Peak areas were calibrated by preparing gravimetric samples in sample bombs. The calibration was continually checked during the course of the entire study.

The pressure in the system was indicated by three (0–300, 0–1000, 0–4000 psia) Heise gages with accuracy 0.1% of the full scale reading.

Temperature was measured by a Leeds and Northrup certified platinum resistance thermometer and reported on the IPTS (1968) scale.

The experimental procedure was the same as used by Elliot. The isotherms were investigated in order of decreasing temperature and increasing pressure. In addition, after an isotherm was completed, additional points were sometimes verified on later dates to verify the consistency of the measurements and to fill the regions of uncertainty.

The bubble-point data were taken after completion of the dew-point investigation. Several experimental dew points were also measured here chromatographically to check the consistency of both experimental procedures. These points, which agreed within the combined accuracy of both experimental procedures, are tabulated in Table I.

An average of 3 h was required to attain steady state, after which at least six analyses were made.

Materials Used

Ultrahigh purity methane with a purity of 99.97 mol % minimum, manufactured by Union Carbide Chemicals Corp., was purchased from IWECO. Research grade *n*-hexane (99.99%) was provided by Phillips Petroleum Co. and was used without further purification. A Model 451 A high-pressure purifier cartridge manufactured by Matheson Gas Products was used in the methane line to remove traces of oil, water, and particles down to approximately 12 μ.

Error Analysis

The error analysis is the same as Elliot's work because the same equipment and experimental procedure technique were used.

The contributing factors are temperature, controlled to 0.02 °C; pressure, measured by Heise gauges calibrated to 0.1% of full scale and controlled within 1 psi; and concentration, determined by chromatography from peak area ratios calibrated to a maximum error of 2% or 0.005 in mole fraction. The vast majority of the data are valid to four significant figures.

The overall error in the dew-point data is either less than 2% or 0.000 01 in mole fraction of *n*-hexane, depending on which is larger.

The maximum error in the resulting K values is 2%.

Results

Experimental results are shown in three tables.

Table I gives the dew points measured by both elution and chromatography methods for comparison purposes. The agreement is satisfactory.

Table II presents all experimental data except in the temperature–pressure region in which only two liquids exist without presence of vapor. The dew points and bubble points are shown along with limiting conditions. Equilibrium constants K are calculated for each component where data are available. Note that this table includes vapor–liquid equilibrium constants at the three-phase conditions. We define these by subscripts on the K to indicate the phases for which the K is calculated, with the third phase indicated outside parentheses. Thus, $(K_{GL_2})_{L_1}$ indicates the vapor–liquid equilibrium constant between the gas G and liquid phase L_2 rich in heavy component (*n*-hexane) with light liquid L_1 rich in light component (methane) present.

The compositions of the two liquids in equilibrium with each other with no vapor present are shown in Table III. Equilibrium constants, κ, defined as the ratio of concentrations of each component in the two liquids, are also reported in this table. Note that the first value at the lowest pressure in each isotherm is at the three-phase condition; hence these values are $(\kappa_{L_1L_2})_G$.

The pressure–composition behavior is given in Figure 1. Note that at −77.24 °C, which is the upper critical solution temperature (UCST), light liquid (L_1) is equal to vapor (G) at p = 755 psia. For $p > 755$ psia, light liquid (L_1') is in equilibrium with heavy liquid (L_2). At −90.69 °C, which is the lower critical solution temperature (LCST), light liquid (L_1') is equal to heavy liquid (L_2) at 495.3 psia. For $p > 495.3$ psia, light liquid (L_1) is in equilibrium with gas (G).

At any given temperature τ between the UCST and LCST, there exists a single fixed pressure Π at which all three phases are present at the same time. At τ for pressures greater than Π up to the respective criticals, only two phases are allowed: L_1–G or L_1'–L_2 depending on the total composition in the equilibrium cell.

In Figure 1, the dashed isobaric lines connect the three phase concentrations, which are equilibrium tie lines for that particular three-phase equilibirum. The dot–dash lines are the loci for L_2 and L_1 with vapor G present. This is a quantitative determination of the schematic Figure 1 lines L_1 and L_2 of ref 7. We must note, however, that we do not agree with the statement in the legend of Figure 1 (*7*) that "Seven of the curves shown in Fig. 3 are the projections of the liquid-phase boundary curves L_1PL_2." These values in Figure 3 of ref 7 must rather be G–L_2 equilibria at concentrations of methane less than the concentration of the LCST and be G–L_1 equilibria at concentrations of methane

Table II. Experimental Data of the Vapor–Liquid Equilibrium of the Methane–*n*-Hexane System

x methane[a]	*y* methane[b]	psia	kPa[c]	*K* methane	*K n*-hexane
		T = 0.01 °C = 32.02 °F = 273.16 K = 427.65 °R			
0.0000	0.0000	0.83[d]	5.72	1120[e]	1.000
0.0097	0.9643	25.1	173.1	99.41	0.03605
0.0196	0.9815	50.1	345.4	50.08	0.1887
0.0387	0.9898	100.1	690.2	25.58	0.01061
0.0567	0.99266	150.1	1034.9	17.51	0.007781
0.0744	0.99396	200.1	1379.6	13.36	0.006525
0.1116	0.99528	300.1	2069.1	8.918	0.005313
0.1469	0.99566	400.1	2758.6	6.778	0.005087
0.2127	0.99578	600	4136.8	4.682	0.005360
0.2742	0.99549	800	5515.8	3.631	0.006214
0.3328	0.99465	1000	6894.7	2.989	0.008019
0.3886	0.99343	1200	8273.7	2.556	0.01075
0.4435	0.99166	1400	9652.6	2.236	0.01499
0.4924	0.9891	1600	11032	2.009	0.02147
0.5400	0.9849	1800	12410	1.824	0.03283
0.5933	0.9797	2000	13789	1.651	0.04991
0.6401	0.9692	2200	15168	1.514	0.08558
0.6564		2300	15857		
0.6949	0.9565	2400	16547	1.376	0.1426
0.7195		2500	17237		
0.7462	0.9400[f]	2550	17582	1.260	0.2364
0.7758	0.9366	2600	17926	1.207	0.2828
0.8025	0.9348[f]	2650	18271	1.165	0.3301
0.9290	0.9290	2675[h]	18443	1.000	1.000
		T = −25.01 °C = −13.02 °F = 248.14 K = 446.65 °R			
0.000	0.0000	0.16[d]	1.1032	8800[e]	1.0000
0.009486	0.98990	20.1	138.58	104.4	0.01020
0.01152	0.99179	25.1	173.06	86.09	0.008306
0.02320	0.99557	50.1	345.43	42.91	0.004535
0.04638	0.99757	100.1	690.16	21.51	0.002548
0.06884	0.99817	150.1	1034.9	14.50	0.001965
0.08998	0.99847	200.1	1379.6	11.10	0.001681
0.1340	0.99872	300.1	2069.1	7.453	0.001478
0.1819	0.99879	400.1	2758.6	5.491	0.001479
0.2595	0.99863	600.1	4136.8	3.848	0.001850
0.3347	0.99820	800	5515.8	2.982	0.002706
0.3998	0.99759	1000	6894.7	2.495	0.004015
0.4672	0.99632	1200	8273.7	2.133	0.006907
0.5252	0.99416	1400	9652.6	1.893	0.01230
0.5804	0.99052	1600	11032	1.707	0.02259
0.6123	0.9889[f]	1700	11721	1.615	0.02863
0.6382	0.9844	1800	12410	1.542	0.04312
0.6937	0.9752	2000	13789	1.406	0.08097
0.7601	0.9644	2200	15168	1.269	0.1484
0.8191	0.9593	2300	15858	1.171	0.2250
0.9564	0.9564	2337	16113	1.000	1.000
		T = −50.00 °C = −58.00 °F = 223.15 K = 401.67 °R			
0.0000	0.0000	0.25[d]	0.1724	32000[e]	1.000
0.01415	0.99841	20.2	139.27	70.56	0.001613
0.01710	0.99872	25.2	173.75	58.41	0.001302
0.03370	0.999343	50.2	346.12	29.65	0.0006799
0.06372	0.999632	100.2	690.85	15.69	0.0003930
0.09213	0.999713	150.2	1035.6	10.85	0.0003161
0.1218	0.999757	200.2	1380.3	8.211	0.0002767
0.1771	0.999775	300.2	2069.8	5.645	0.0002734
0.2294	0.999755	400.2	2759.3	4.358	0.0003179
0.3282	0.999594	600	4136.8	3.046	0.0006043
0.4207	0.999256	800	5515.8	2.375	0.001284
0.4952	0.99851	1000	6894.7	2.016	0.002952
0.5893	0.99613	1200	8273.7	1.690	0.009423
0.6518	0.99013	1400	9652.6	1.519	0.02835
0.7011	0.9871	1500	10342	1.408	0.04316
0.7423	0.9841	1600	11032	1.326	0.06170
0.7774	0.9816	1700	11721	1.263	0.08266
0.8022		1750	12066		
0.8189		1775	12238		
0.8444		1790	12342		
0.8522		1800	12410		
0.8922		1803	12431		
0.9784	0.9784	1804[h]	12438	1.000	1.000

Table II (continued)

x methane[a]	y methane[b]	psia	kPa[c]	K methane	K n-hexane
		$T = -63.00$ °C = −81.40 °F = 210.15 K = 378.27 °R			
0.0000	0.0000	0.008[d]	0.0552	76000[e]	1.000
0.01563	0.999495	20.2	139.27	63.95	0.0005130
0.01867	0.999589	25.2	173.75	53.54	0.0004188
0.03782	0.999781	50.2	346.12	26.44	0.0002276
0.07307	0.999868	100.2	690.85	13.68	0.0001424
0.1079	0.999888	150.2	1035.6	9.264	0.0001256
0.1411	0.999903	200.2	1380.3	7.087	0.0001129
0.2071	0.999894	300.2	2069.8	4.828	0.0001337
0.2700	0.999878	400.2	2759.3	3.703	0.0001671
0.3881	0.999798	600	4136.8	2.576	0.0003301
0.5139	0.999402	800	5515.8	1.945	0.001230
0.6162	0.99730	1000	6894.7	1.618	0.007036
0.7156	0.99177	1200	8273.7	1.386	0.02894
0.7576		1300	8963.1		
0.8091	0.9882	1400	9652.6	1.221	0.06181
0.8279		1420	9790.5		
0.8568		1435	9893.9		
0.8713		1440	9928.4		
0.9872	0.9872	1443[h]	9949.1	1.000	1.000
		$T = -75.10$ °C = −103.18 °F = 198.05 K = 356.49 °R			
0.0000	0.0000	0.002[d]	0.0138	200000[e]	1.000
0.01950	0.999848	19.9	137.21	51.28	0.000155
0.02438	0.999885	25.0	172.37	41.02	0.000118
0.04742	0.999927	50.0	344.74	21.09	0.0000766
0.09603	0.999949	100.0	689.47	10.41	0.0000564
0.1390	0.999955	150.0	1034.2	7.194	0.0000523
0.1813	0.999952	200.0	1378.9	5.515	0.0000586
0.2660	0.999939	300.0	2068.4	3.760	0.0000831
0.3412	0.999919	400.0	2757.9	2.931	0.000123
0.4225	0.999893	500.0	3447.4	2.367	0.000185
0.5076	0.999832	600.0	4136.8	1.970	0.000341
0.5936	0.999640	700	4826.3	1.684	0.000886
0.6872	0.99789	800	5515.8	1.452	0.00675
0.7596	0.99572	900	6205.3	1.311	0.0178
0.8117	0.99435	1000	6894.7	1.225	0.0300
0.8468		1050	7239.5		
0.8932		1055	7273.9		
0.99364	0.99364	1057[h]	7287.7	1.000	1.000
		$T = -77.24$ °C = −107.03 °F = 195.91 K = 352.64 °R			
0.0000		0.007[d]	0.048		
0.02082		20.0	137.89		
0.04831		50.0	344.74		
0.09528		100	689.47		
0.1407		150	1034.2		
0.1849		200	1378.9		
0.2698		300	2068.4		
0.3555		400	2757.9		
0.4429		500	3447.4		
0.5323		600	4136.8		
0.6422		700	4826.3		
0.7177	0.99763	755[i]	5205.5	1.390	0.00840
		$T = -80.00$ °C = −112.00 °F = 193.15 K = 347.60 °R			
0.0000	0.0000	0.0013[d]	0.00896	280000[e]	1.000
0.02210	0.999905	20.1	138.58	45.25	0.0000972
0.02728	0.999932	25.1	173.06	36.65	0.0000699
0.09964	0.999964	100.1	690.16	10.04	0.0000400
0.2851	0.999970	300.1	2069.1	3.508	0.0000420
0.4697	0.999932	500.1	3447.4	2.129	0.000128
0.5802	0.999830	600	4136.8	1.723	0.000405
0.6902	0.999567	675	4653.9	1.448	0.00140
0.7239	0.999393	692[i]	4771.2	1.381	0.00220
0.9864 (L_1)	0.999393	692[i]	4771.2	1.013	0.0446
0.9914 (L_1)	0.99898	700	4826.3	1.008	0.119
0.9988 (L_1)	0.99882	708[i]	4881.5	1.000	1.000
		$T = -82.65$ °C = −116.77 °F = 190.50 K = 342.90 °R			
0.0000	0.0000	0.00093[d]	0.00641	350000[e]	1.000
0.02256	0.999924	20.0	137.89	44.33	0.0000778
0.02803	0.999960	25.0	172.37	35.68	0.0000412
0.1047	0.999970	100.0	689.47	9.548	0.0000335

Table II (continued)

x methane[a]	*y* methane[b]	psia	kPa[c]	K methane	*K* *n*-hexane
0.3004	0.999988	300.0	2068.4	3.329	0.0000172
0.5041	0.999907	499.6	3444.6	1.984	0.000188
0.6487	0.999814	600	4136.8	1.541	0.000529
0.7438	0.999611	638[f]	4398.8	1.344	0.00152
0.9695 (L_1)	0.999611	638[f]	4398.8	1.031	0.0128
0.9724 (L_1)	0.999577	645[f]	4447.1	1.028	0.0153
0.9745 (L_1)	0.999587	650	4481.6	1.026	0.0162
0.9897 (L_1)	0.999609	655	4516.1	1.010	0.0380
0.9919 (L_1)	0.999687	660	4550.5	1.008	0.0386
0.999847 (L_1)	0.99847	665[h]	4565.0	1.000	1.000
		T = −86.92 °C = −124.46 °F = 186.23 K = 335.21 °R			
0.0000		0.00054[d]	0.00372		
0.06129		50.0	344.74		
0.1189		100	689.47		
0.1813		150	1034.2		
0.2357		200	1378.9		
0.3412		300	2068.4		
0.4593		400	2757.9		
0.6010		500	3447.4		
0.6826		540	3723.2		
0.8057	0.999837	559[f]	3854.1	1.241	0.000839
0.9505 (L_1)	0.999837	559[f]	3854.1	1.052	0.00329
0.9776 (L_1)		574	3957.6		
0.9871 (L_1)		579	3992.0		
1.000 (L_1)		582[g]	4012.7		
		T = −90.69 °C = −131.24 °F = 182.46 K = 328.43 °R (LCST)			
0.0000		0.00034[d]	0.00234		
0.02766		20.0	137.89		
0.03463		25.0	172.37		
0.06623		50.0	344.74		
0.1308		100	689.47		
0.1907		150	1034.2		
0.2560		200	1378.9		
0.3822		300	2068.4		
0.5178		400	2757.9		
0.6100		450	3102.6		
0.7426		480	3309.5		
0.9286	0.999946	495.3[f]	3414.9	1.077	0.000756
0.9640 (L_1)		510	3516.3		
0.9876 (L_1)		515	3550.8		
1.000 (L_1)		516[g]	3557.7		

[a] All liquid-phase data are L_2 unless otherwise noted. [b] Vapor compositions from Chen et al. (*5*), except as noted by *f*. [c] Pa: Pascal = kg/m s^2 = N/m^2; 1 psia = 6.8947 kPa. [d] Vapor pressure of *n*-hexane from Carruth (*2*). [e] $K_{CH_4}^{\infty}$. [f] Dew points measured by chromatography. [g] Vapor pressure of CH_4. [h] Critical pressure where liquid ≡ gas. [i] Pressure at which L_1–L_2–G exists.

Table III. Liquid–Liquid Equilibrium Data of the Methane–*n*-Hexane System[a]

x methane (L_2)	*x'* methane (L_1')	psia	kPa	κ methane	κ *n*-hexane
	T = −77.24 °C = −107.03 °F = 195.91 K = 352.64 °R (UCST $L_1 \equiv G$)				
0.7177	0.9976	755[c]	5205.5	1.3900	0.008502
0.7425	0.9851	800	5515.8	1.3267	0.05786
0.7701	0.9769	850	5860.5	1.2685	0.1005
0.7809	0.9674	880	6067.4	1.2388	0.1488
0.7950	0.9520	910	6274.2	1.1975	0.2342
0.8151	0.9390	950	6550.0	1.1520	0.3840
0.8416	0.9133	975	6722.4	1.0852	0.5474
0.8900[b]	0.8900[b]	986[d]	6798.2	1.000	1.000
	T = −80.00 °C = −112.00 °F = 193.15 K = 347.67 °R				
0.7239	0.9864	692[c]	4771.2	1.3626	0.04926
0.7415	0.9785	720	4964.2	1.3196	0.08317
0.7531	0.9716	740	5102.1	1.2901	0.1150
0.7649	0.9660	760	5240.0	1.2629	0.1446
0.7858	0.9522	800	5515.8	1.2118	0.2232
0.7949	0.9445	820	5635.7	1.1882	0.2706
0.8098	0.9377	840	5791.6	1.1579	0.3276

Table III. (continued)

x methane (L_2)	x' methane (L_1')	psia	kPa	κ methane	κ n-hexane
0.8278	0.9238	860	5929.5	1.1160	0.4425
0.9004	0.9004	883[d]	6088.1	1.000	1.000
	T = −82.65 °C = −116.77 °F = 190.50 K = 342.90 °R				
0.7438	0.9695	638[c]	4398.8	1.3034	0.1191
0.7756	0.9631	675	4653.9	1.2418	0.1644
0.7829	0.9486	700	4826.3	1.2117	0.2368
0.8042	0.9369	725	4998.7	1.1650	0.3223
0.8071	0.9484	730	5033.1	1.1751	0.2675
0.8297	0.9280	760	5240.0	1.1185	0.4228
0.8975	0.8975	770[d]	5308.9	1.000	1.000
	T = −86.92 °C = −124.46 °F = 186.23 K = 335.21 °R				
0.8057	0.9505	559[c]	3854.2	1.1797	0.2548
0.8199	0.9412	580	3998.9	1.1479	0.3265
0.8313	0.9335	600	4136.8	1.1229	0.3942
0.8515	0.9246	612	4219.6	1.0858	0.5077
0.9013	0.9013	624	4302.3	1.000	1.000
	T = −90.69 °C = −131.24 °F = 182.46 K = 328.43 °R (LCST $L_1' \equiv L_2$)				
0.9286	0.9286	495.3[c]	3414.9	1.000	1.000

[a] Except at pressure indicated with footnote *c*, no gas phase is present. [b] Estimated value. [c] L_1–L_2–G. [d] $L_1 \equiv L_2$.

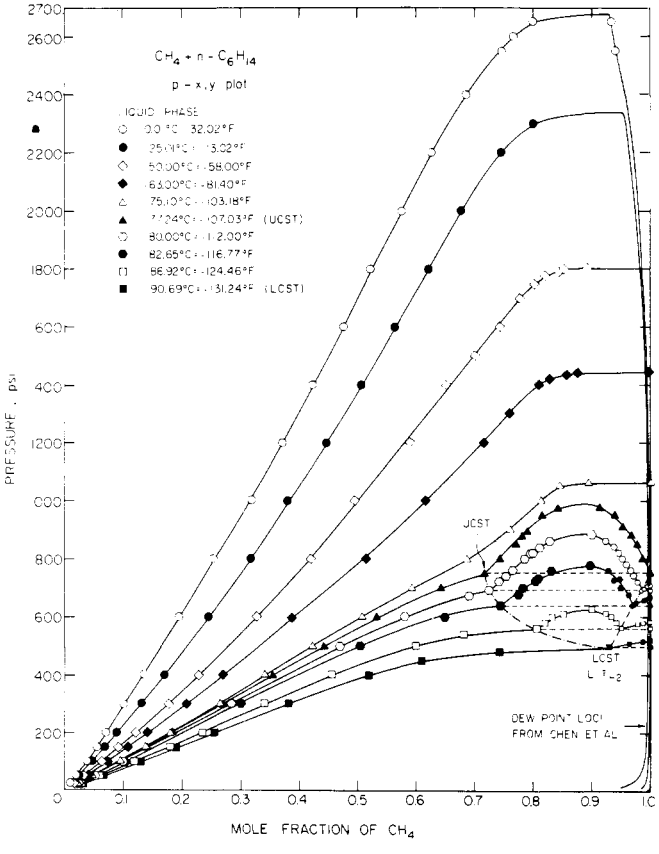

Figure 1. Pressure–composition diagram for the methane–*n*-hexane system.

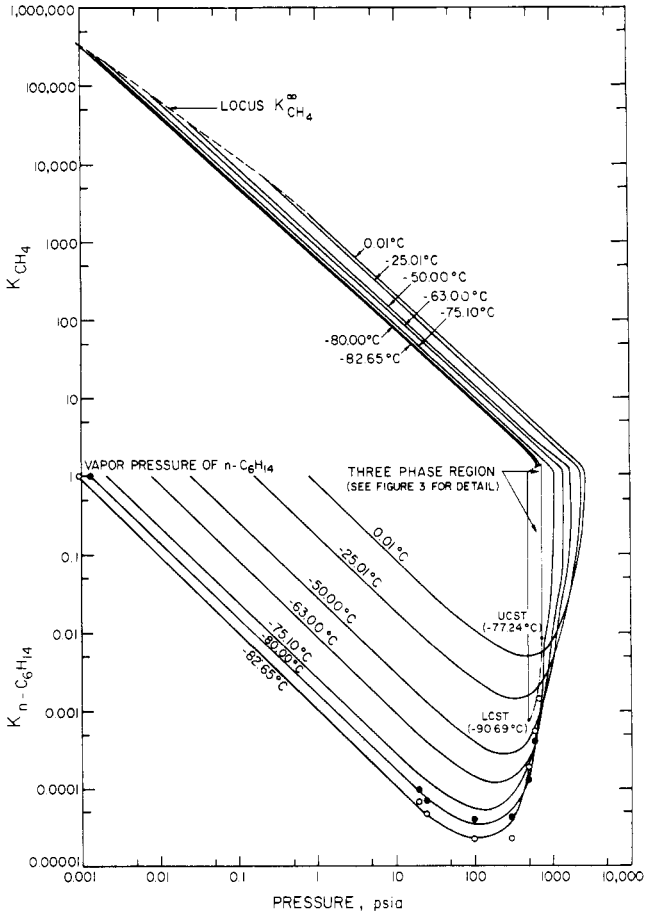

Figure 2. *K* value vs. pressure along isotherms for the methane–*n*-hexane system.

greater than the LCST. Nevertheless, the technique of Davenport and Rowlinson (*7*) does yield a value for the LCST quite close to our value: 182.6 K and 0.30 weight fraction *n*-hexane (0.926 mole fraction methane) as compared to our −90.69 °C (182.46 K) and 0.9286 mole fraction methane.

Note also that for the isotherm at −75 °C, which is slightly more than 2 °C above the UCST, the shape of the *p*–*x* plot is affected.

K values for each temperature as a function of pressure are shown in Figure 2. Comparisons with BWRS equation predictions are good in general (*10*). Larger deviations occur at lower temperatures and pressures near critical.

Figure 3 reveals the details of the equilibrium constants between the UCST and LCST. *K* values and κ values are put together for each isotherm as a function of pressure in an expanded scale. The dot–dash lines are the respective loci for the

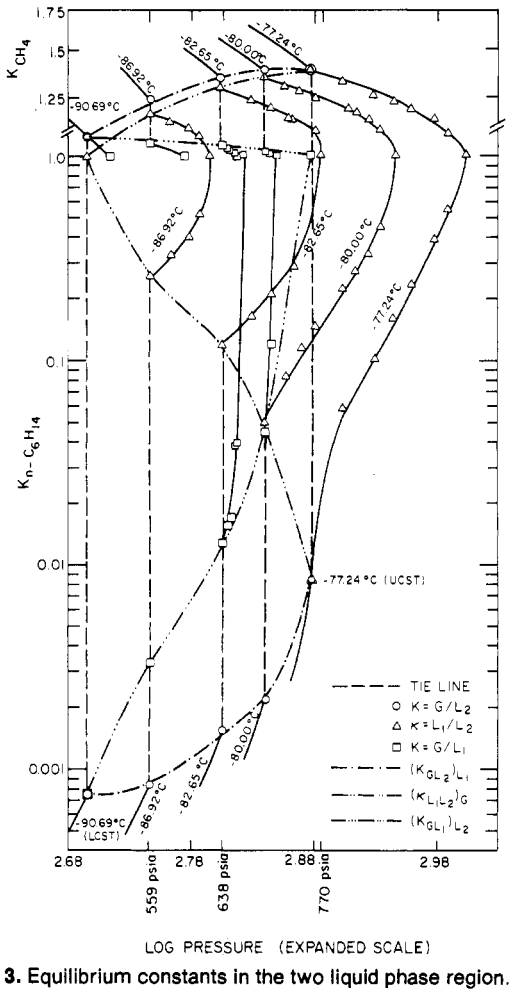

Figure 3. Equilibrium constants in the two liquid phase region.

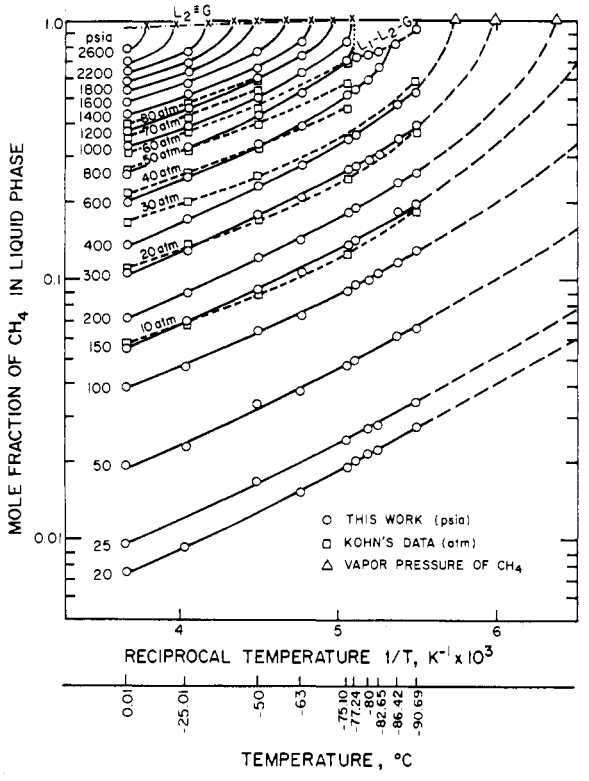

Figure 4. Isobaric bubble point behavior for the methane–*n*-hexane system.

equilibrium constants at the three phase conditions. These correspond to the dot–dash lines on Figure 1.

Cross plots of isobaric concentration vs. reciprocal absolute temperature are shown in Figure 4. Shim and Kohn's data (*11*) are also shown for comparison.

Acknowledgment

Mr. Ray Martin provided invaluable assistance in the construction and maintenance of the equipment.

Glossary

K	ratio of vapor concentration to liquid concentration
κ	ratio of light liquid concentration to heavy liquid concentration
x	liquid concentration, mole fraction
y	vapor concentration, mole fraction
∞	superscript denoting limiting value for the subscripted component at the limiting other pure component vapor pressure
L_1	light liquid in equilibrium with vapor
L_1'	light liquid in equilibrium with heavy liquid
L_2	heavy liquid in equilibrium with vapor or L_1'
G	gas phase in equilibrium with liquid
τ	temperature in three-phase region
Π	pressure in L_1–L_2 or L_1–G regions

Literature Cited

(1) Boomer, E. H., Johnson, C. A., *Can. J. Res.*, **16B,** 328 (1938).
(2) Carruth, G. F., Kobayashi, R., *J. Chem. Eng. Data,* **18,** 115 (1973).
(3) Chen, R. J. J., Chappelear, P. S., Kobayashi, R., *J. Chem. Eng. Data,* **19,** 53 (1974).
(4) Chen, R. J. J., Chappelear, P. S., Kobayashi, R., *J. Chem. Eng. Data,* **19,** 58 (1974).
(5) Chen, R. J. J., Chappelear, P. S., Kobayashi, R., *J. Chem. Eng. Data,* **21,** 213 (1976).
(6) Chu, T. C., Chen, R. J. J., Chappelear, P. S., Kobayashi, R., *J. Chem. Eng. Data,* **21,** 41 (1976).
(7) Davenport, A. J., Rowlinson, J. S., *Trans. Faraday Soc.*, **59,** 78 (1963).
(8) Elliot, D. G., Chen, R. J. J., Chappelear, P. S., Kobayashi, R., *J. Chem. Eng. Data,* **19,** 71 (1974).
(9) Poston, R. S., McKetta, J. J., *J. Chem. Eng. Data,* **11,** 362 (1966).
(10) Private communications with Exxon Product Research Co. (1976).
(11) Shim, J., Kohn, J. P., *J. Chem. Eng. Data,* **7,** 3 (1962).

Received for review December 20, 1976. Accepted May 19, 1977. Presented at the 69th Annual Meeting of AIChE, Chicago, Ill., Nov 1976. Financial support was provided by the Gas Processors Association and The American Gas Association.